International Journal of Natural and Engineering Sciences 4 (1): 81-93, 2010
ISSN: 1307-1149, E-ISNN: 2146-0086, www.nobel.gen.tr

Evaluation of the Constant Modulus Algorithm Application

H. Shirzad[1] J. Poorahmadazar[1] Ch.Ghobadi[1] J.Nourinia[1]

[1] Department of Electrical Engineering Islamic Azad University of Urmia branch, Urmia, West Azarbayjan, Iran

Corresponding author
E-mail: hamedeshirzad@gmail.com

Received : November 12, 2009
Accepted : January 30, 2010

Abstract

The convergence behavior of the Least Squares Constant Modulus Algorithm in an adaptive beam forming application is examined. It is assumed that the desired signal and the interfer¬ence are uncorrelated. The improvement in output SIR with each iteration of the algorithm is predicted for several different signal environments. Deterministic results are presented for an environment containing two complex sinusoids. Probabilistic results are presented for a constant modulus desired signal with a constant modulus interferer and with a Gaussian interferer. The asymptotic improvement in output SIR as the output SIR becomes high is also derived. The results of Monte Carlo simulations using sinusoidal, FM, and QPSK signals are included to support the derivations.

Keywords: Adaptive, Algorithm, Monte Carlo, Constant Modulus.

INTRODUCTION

We will study a member of the class of adaptive algorithms generally known as Godard or Constant Modulus Algorithms (CMA) [1,2]. These algorithms can be used for adaptive beam forming, equalization, and other applications when the desired signal has a constant envelope. Examples of such signals include FM, PSK, and FSK. The CMA can also be applied to many non-CM signals (e.g., pulse-shaped PSK, QAM) although the performance may be degraded relative to the case where the desired signal is CM [3,4]. The main advantage of CMA is that it is a 'blind' adaptive algorithm, i.e., it does not require a training signal. Other blind adaptive algorithms have been designed to exploit cyclostationarity [5,6,7], known signal constellation [8], known spreading code in CDMA [9], and time or frequency gated properties [10,11,12].The first CMA to be proposed was based on a Stochastic Gradient Descent (SGD) form [2]. The main drawback of this method is its slow convergence. A faster converging CMA similar in form to the Recursive Least Squares method is the orthogonal zed CMA [13]. Another fast converging CMA is the Least Squares CMA (LSCMA)[14,6], which is a block-update iterative algorithm. It is guaranteed to be stable and is easily implemented. Despite the generally accepted use of the LSCMA, few analytical results on its convergence have appeared in the open literature. The performance of the algorithm has instead been demonstrated through Monte Carlo simulation. The lack of analytical results is due to the difficulty of analyzing the non-linear CMA cost function. Existing work on the convergence behavior of CMA mostly deals with finding minima of the CMA cost function and finding undesirable stable equilibrium in equalization applications (e.g., see [15,16] and references therein). A notable exception is the work by Treichler and Larimore on convergence of SGD CMA in an environment containing two complex sinusoids [10]. Their work predicts the output power of each sinusoid in a temporal filtering application. The Analytic CMA (ACMA) algorithm presented by van der Veen in [14] should also be noted. This algorithm solves directly for a set of beam former weight vectors that spatially separate a set of CM signals. The ACMA, although effective in many situations, is fairly complex and its behavior with closely spaced and/or low SNR signals is not clear. For these reasons it is recommended in [14] that the ACMA be used to initialize the LSCMA, and that several iterations of the LSCMA be used to find the optimal solutions for the weight vectors. In this paper we determine the convergence rate of the LSCMA in some simple environments, including: (i) high output SIR; (ii) sinusoidal desired signal and sinusoidal interferer; (iii) CM desired signal and CM interferer; (iiii) CM desired signal and Gaussian interferer. We assume that the interference is uncorrelated with the

desired signal. The convergence rate is expressed in terms of the SIR improvement achieved with one iteration of the LSCMA. We first examine the situation where the LSCMA output SIR is high We show that if the interference is perfectly removable, each LSCMA iteration will increase the output SIR by approximately 6 dB. This result is valid for any CM desired signal (arbitrary angle modulation), and any uncorrelated interference. We next examine an environment containing two complex sinusoids, and show that the LSCMA output SIR can be predicted for each iteration. The results are analogous to those presented in [10]. An environment containing two CM signals, each having random phase, is then considered. It is shown that the average behavior of the LSCMA in this environment is similar to the deterministic behavior in the two-sinusoid environment. Finally, an environment containing a CM desired signal and Gaussian interference is examined.

Overview of LSCMA System

The objective of the adaptive beam former is to obtain a high-quality estimate of a desired signal in the presence of co channel interference using an array of antennas. Letting the *M* x 1 vector x(*n)* represent the signals and noise received at an array of *M* antennas at discrete time index *n* gives

$$X(n)=\sum_{i=1}^{L} a i s_i(n) + q(n) \quad (1)$$

where the *M* x 1 vector a, is the spatial signature corresponding to signal *s(n)* and the *M* x 1 vector *q(n)* contains environmental and receiver noise. The model defined by Eq.(1) is often referred to as the narrowband model, since it is assumed that the signals are narrowband relative to the carrier frequency. The signals are also assumed to have unit variance and to be temporally uncorrelated with each other and with the background noise. That is

$$\varepsilon\{s_i(\varepsilon\{s_i(n)\, s_i(\, s_i(n)\}=\begin{cases}1 & if\ i=j\\ 0 & if\ i\neq j\end{cases} \quad (2)$$

where $\varepsilon\varepsilon\{.\}$ denotes expectation. The signal power is incorporated in the spatial signature, which describes the amplitude and phase difference between the signal received at a reference antenna and all other antennas. In the absence of multi path, the spatial signature is generally referred to as an array response vector. The array response vector is dependent on the angle of arrival (AOA) of the signal, the array geometry, the gain pattern of each antenna, the carrier frequency of the incident signals, etc. When a signal is incident from more than one direction the spatial signature will be a linear combination of the array response vectors corresponding to the AOA of each path. This assumes that the multipath delay spread *T* is small relative to 1/ *B,* where *B* is the signal bandwidth. If *T* > 1/ *B,* each multipath component received by the array is uncorrelated with other arriving components, and each component is treated as a different signal. The case in which the delay spread is significant, but not so large that the multipath arrivals are uncorrelated, is not treated in this paper. An adaptive beamformer weights and sums the signals received by the array to form an estimate $y(n) = W^H x(n)$ of the desired signal, where w is the *M* x 1 complex vector of beam former weights and w^H is, as usual, the Hermitian transpose. The desired behavior of adaptive beam forming is most easily visualized for environments that lack multi path. In these environments an adaptive beam former seeks to steer a beam towards the AOA of the desired signal while simultaneously steering nulls towards the AOA's of the interfering signals. Computation of the optimal (maximum output SNR, minimum MSE, etc.) weight vector requires either a training signal or precise knowledge of the desired signal spatial signature. In practice, a training signal is not always available. Furthermore the spatial signature may be impractical to obtain. In such situations the CMA may be used to obtain a nearly optimal weight vector if the desired signal has constant modulus. The constant modulus property can in general be exploited by minimizing the non-linear cost function

$$F_{(p,q)} =< (|y(n)|-1)^2 > \quad (3)$$

where < . > denotes time average. The form of Eq.(3) generally makes analysis of CMA difficult. The LSCMA is a block update iterative technique for minimizing the $F_{(1,2)}$ cost function given by:

$$F_{(1,2)} =< (|y(n)|-1)^2 > \quad (4)$$

The LSCMA is implemented as follows. At the kth iteration, *N* temporal samples of the beam former output are generated using the current weight vector W_k. This gives:

$$y_k(n) = W_k^H x(n) \quad (5)$$

The initial weight vector $w_0 w_0$ can be taken as w_0= $[1\ 0\ 0\ \ldots 0\ ]^T$if no a-priori information is available. Other initialization methods are considered in [11], where it is shown that the dominant eigenvectors of the observed data covariance matrix are good choices for initial weight vectors. The kth signal estimate is then hard limited to yield

$$d_k d_k(n)=\frac{y_k(n)}{|y_k(n)|} \quad (6)$$

and a new weight vector is formed according to

$$W_{k+1} = R_{xx}^{-1} r_{xd} \quad (7)$$

Where $$R_{xx} =< x(n)\, x^H(n) >_N \quad (8)$$

And $$r_{xd} =< x(n)\, d_k^*(n) >_N \quad (9)$$

In the above expressions,$<.>_N$ denotes a time average over $0 \leq n \leq N-1$. The updated weight vector W_{k+1} minimizes the mean square error

$$< |d_k(n) - W_{k+1}^H x(n)|^2 >_N \quad (10)$$

The iteration described by Eq.(5), Eq.(6), and Eq.(7) is continued until either the change in the weight vector is smaller than some threshold, or until the envelope variance of the output signal is deemed sufficiently small. In a stationary environment, the LSCMA iteration can be performed using a new block of data, or can be re-applied to the same block of observed data. The former approach is referred to as *dynamic* LSCMA in [13], while the latter approach is referred to as *static* LSCMA. The only parameter which must be selected when using the LSCMA is the block size *N*. Selection of *N* will depend on many factors, including the acceptable latency of the update procedure, the rate at which the signal environment is changing, and the available processing power. Also, the number of temporal samples of array data must be equal to or greater than the number of antennas so that the linear system of equations is over determined. The LSCMA block size is similar to the SGD adaptation step parameter in that smaller block sizes yield faster convergence at the cost of higher variance in the output SNR. By faster convergence we mean that fewer temporal samples of data need be processed to achieve steady-state. An interesting feature of the LSCMA is that the output SIR as a function of the number of iterations is nearly independent of data block size. That is, the LSCMA typically converges in 5 to 10 iterations regardless of the block size.An aside is in order here on the computational complexity of the LSCMA. Direct minimization of MSE by solving a set of simultaneous linear equations, as in Eq.(7), is often considered impractical for real-time applications because of the computational load. Certainly this may be true for adaptive equalization applications, where the number of filter coefficients can be large. However, the computational load is more reasonable for beam forming applications since adaptation of a relatively small number of coefficients is required. The LSCMA bears a strong resemblance to the classical least squares method that can be used when a known training signal is available. The LSCMA can be interpreted as a least squares method that uses a pseudo-training signal that is derived from the observed data. This is the viewpoint taken here. We essentially determine the quality of the pseudo-training signal in some representative situations. A different motivation for the LSCMA is presented next, along with a discussion of the relationship of the LSCMA to other existing algorithms. The LSCMA can be viewed as a method where a signal estimate is alternately projected onto the set of CM signals and the space spanned by the observed data. In this way the LSCMA resembles the Gerchberg-Saxton algorithm (GSA) [12], as noted by Wang, et al. [5] and Van der Veen [14]. The problem solved by GSA is to recover the magnitude and phase of a signal when only the magnitude of the signal and the magnitude of its Fourier transform are known. This problem arises in many applications, including speech and image processing (see,[15]). The GSA projects a signal estimate in an alternating fashion onto time domain and frequency domain property sets. The principal similarity of GSA and LSCMA is that both employ a projection onto a non-convex set. This is in contrast to Projections Onto Convex Sets (POCS) [1,6,7,9]. POCS can be used to find a signal estimate which satisfies multiple properties. The POCS takes an initial signal estimate and projects it in an alternating fashion onto the various property sets being exploited. The POCS is guaranteed to converge when the sets are closed and convex. The GSA and the LSCMA can be viewed as belonging to a class of algorithms that are sometimes known as the Method of Generalized Projections (MGP). The GSA is the archetype of MGP, and some authors use 'Gerchberg-Saxton' as a generic term to describe any MGP. MGP convergence cannot be assured in general, although in some cases MGP exhibits the 'error reduction' property. This implies that each iteration of a MGP reduces, or at worst does not increase, the cost function being minimized. The error reduction property of the LSCMA is described in the original LSCMA paper [13], but the relationship of the LSCMA to the GSA and other MGP approaches was not recognized.

Analysis Frameworks

In this section we describe the general framework used to analyze the LSCMA. A key assumption is that the interference is uncorrelated with the desired signal. We essentially describe a simple way to measure the quality of the pseudo-training signal, *d(n)*. If no background noise is present, the quality of the beamformer output *y(n)* will be identical to the quality of *d(n)*. When background noise is present, the quality of *y(n)* is dependent on the quality of *d(n)* and the optimal output SINR. The optimal output SINR is in turn dependent on many factors, including the array geometry, the number of antennas, the number of incident signals, and the angle of arrival of each signal. The beamformer output signal at the kth iteration can be expressed, to within a multiplicative constant, as

$$y_k(n) = W_k^H(n) = s(n) + gz(n) \quad (11)$$

where *s(n)* is the constant modulus desired signal, *z(n)* is noise and interference, and the SINR of the beamformer output is controlled by *g*. Both the desired signal *s(n)* and the interference *z(n)*

have unit variance. The hard-limiter output $d_k(n)$ will contain three components: (i) one component which is correlated with the desired signal; (ii) one component which is correlated with the interference; and (iii), one component which is correlated with neither the signal nor the interference. This last component is the result of intermodulation. between the signal and the interference. We can express the hard-limiter output as

$$d_k(n)=\frac{y_k(n)}{|y_k(n)|}=\propto s(n)+\beta z(n)+\varepsilon(n) \quad (12)$$

Where the scalars $\propto$ and β control the desired signal power and the interference power, respectively, and $\varepsilon(n)$ contains the intermodulation terms. We will now examine the relationship between the SINR in $d_k(n)$ and the SINR in the updated beam former output y_{k+1}. We initially assume that no background noise is present, and that the array has sufficient degrees of freedom to completely remove the interference. Given these assumptions, the optimal beam former output SINR is infinite. These assumptions are clearly not realistic, but this helps provide insight into the behavior of the LSCMA. As the block size N→ ∞, the updated weight vector W_{k+1}minimizes the MSE between $y_{k+1}(n)$ and $d_k(n)$,

$$lim_{n\to\infty}\frac{1}{N}\sum_{n=0}^{N-1}|y_{k+1}(n)-d_k(n)|^2 = \varepsilon\{|y_{k+1}(n)-d_k(n)|^2\} \quad (13)$$

We can express the updated beamformer output as

$$y_{k+1}(n)=W_{k+1}^H x(n)=\alpha' s(n)+\beta' z(n) \quad (14)$$

Which, together with Eq.(12), allows the MSE to be written as

$$\varepsilon\{|y_{k+1}(n)-d_k(n)|^2\} = \varepsilon\{|(\alpha'-\alpha)s(n)+(\beta'-\beta)z(n)-\xi(n)|^2\} \quad (15)$$

$$=|\alpha'-\alpha|^2\sigma_s^2+|\beta'-\beta|^2\sigma_z^2 \quad (16)$$

where we have made use of the fact that $s(n)$, $z(n)$, and $\xi(n)$ are mutually uncorrelated. Clearly the MSE is minimized for $\alpha'=\alpha$, $\beta'=\beta$. This implies that the signal component in the updated beamformer output will match the magnitude and *phase* of the signal component in the hard-limiter output. Thus the MSE between $d_k(n)$ and the updated beamformer output $y_{k+1}(n)$ is minimized when

$$y_{k+1}(n)=W_{k+1}^H x(n)=\alpha s(n)+\beta z(n) \quad (17)$$

In order to find α andβ, we calculate the cross-correlation of $s(n)$ and $z(n)$, respectively, with $d(n)$. Note that

$$R_{sd}\triangleq\varepsilon\{s(n)d^*(n)\} \quad (18)$$

$$=\varepsilon\{s(n)(\alpha s(n)+\beta z(n)+\xi(n))\} \quad (19)$$

$$=\alpha^* \quad (20)$$

Similarly we have

$$R_{zd}\triangleq\varepsilon\{s(n)d^*(n)\}=\beta^* \quad (21)$$

The SINR ρ in the hard-limiter output d_k is

$$\rho(d_k)=\frac{|\alpha|^2}{|\beta|^2}=\frac{|R_{sd}|^2}{|R_{zd}|^2} \quad (22)$$

since we model $s(n)$ and $z(n)$ as having unit variance. Thus, the output SIR of the updated LSCMA weight vector can be determined from R_{sd} and R_{zd}. This requires that the probability density function (PDF) of the signal and the interference be known. To further illustrate the concepts behind this analysis framework, we will apply the LSCMA to a simple environment containing two uncorrelated complex sinusoids. The array configuration consists of two antennas, with the interelement spacing equal to $\lambda/2\lambda/2$, where $\lambda\lambda$ is the carrier wavelength. One sinusoid, with a frequency of 5/1024, is incident from broadside to the array, which we define as 0°. This sinusoid is treated as the desired signal. The second sinusoid, with a frequency of 31/1024, is incident from 30°. This sinusoid is treated as the interfering signal. The amplitude of the first sinusoid is unity, and the amplitude of the second sinusoid is 0.9. The LSCMA is applied to this environment with the initial weight vector Wo = [1 0]. Thus the initial SIR is approximately -0.9 dB. The LSCMA block size N is set to 1024 samples. The period gram of the initial beamformer output y_0(n) is shown in Figure 1. The next step in the LSCMA is to hard-limit the beamformer output. The period gram of the hard-limited beamformer output is shown in Figure 2. Note that the original sinusoidal frequencies are still present, along with intermodulation products. Also note that the relative amplitude of the desired sinusoid is now slightly higher relative to the interfering sinusoid. The exact change in relative amplitude is calculated later in Subsection III. The next step in the LSCMA is to update the weight vector using the hard-limiter output in the same manner as a training signal. Figure 3 shows the period gram of the updated beamformer output. As discussed earlier, the amplitude of each sinusoid in the updated beamformer output matches

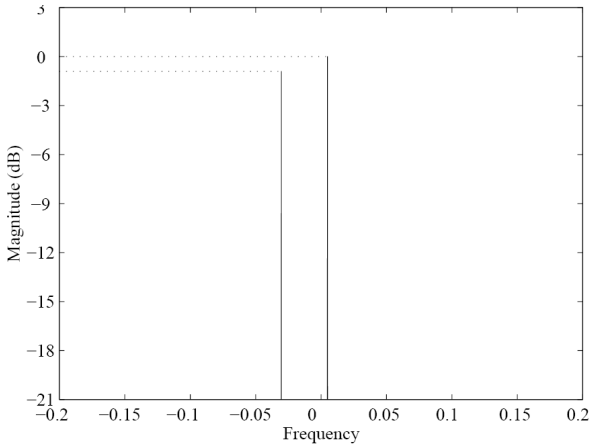

Figure 1: Periodogram of the initial beamformer output for the simple two-sinusoid environment. The initial SIR of 0.9 dB is indicated by the dotted horizontal lines.

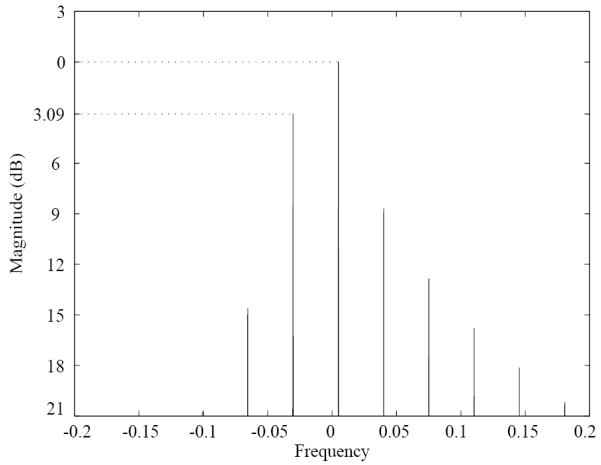

Figure2: Periodogram of the hard-limited beamformer output for the simple two-sinusoid environment. The SIR of 3.09 dB is indicated by the dotted horizontal line.

the amplitude of the corresponding sinusoids in the hard-limiter output. The intermodulation products are orthogonal to the signals present in the array data, and so have no effect on the weight update. It can be seen that the SIR in the updated beamformer output is approximately 3 dB higher than the initial SIR.

Note that the calculation of SIR does *not* take into account the intermodulation terms. When background noise is present the interference and noise cannot be completely removed by beam forming. Independent thermal noise generated by each of the *M* receivers required for the *M* antennas in the array is a *common* source of background noise.

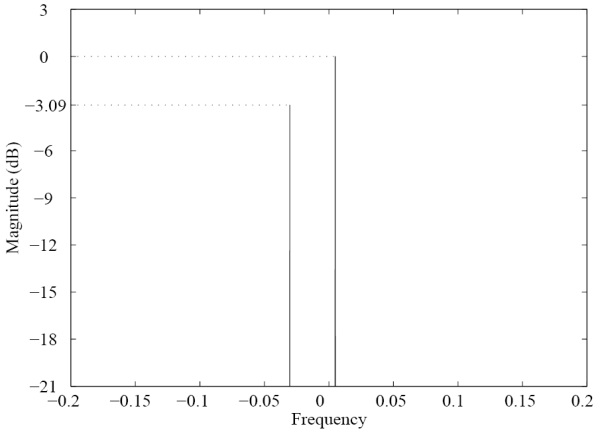

Figure 3: Periodogram of the updated beamformer output for the simple two-sinusoid environment. The SIR of 3.09 dB is identical to the SIR in the hard-limiter outputs.

The relationship between the SINR in $d_k(n)$and the updated LSCMA output SINR is then somewhat more complicated. We now derive an expression for the output SINR of the updated LSCMA weight vector when background noise is present. This will be shown to be dependent only on the optimal output SINR, the initial SINR, and the SINR gain provided by the hard limit non-linearity. The observed data is modeled as When background noise is present the interference and noise cannot be completely removed by beam forming. Independent thermal noise generated by each of the *M* receivers required for the *M* antennas in the array is a *common* source of background noise. The relationship between the SINR in $d_k(n)$and the updated LSCMA output SINR is then somewhat more complicated.We now derive an expression for the output SINR of the updated LSCMA weight vector when background noise is present. This will be shown to be dependent only on the optimal output SINR, the initial SINR, and the SINR gain provided by the hard limit non-linearity. The observed data is modeled as

$$x(n) = as(n) + q(n) \tag{23}$$

Where a is the spatial signature of the desired signal and q(*n)* contains the noise and interference. We assume that R_{qq} is equal to the identity matrix. There is no loss of generality since whitening the data has no effect on the LSCMA. The cross-correlation vector R_{xd} is given by

$$R_{xd} = caa^H W_0 + W_0 \tag{24}$$

where W_0 is the initial weight vector, and c is the square root of the SINR gain, with Eq.25 The covariance matrix of the data is

$$c \triangleq \frac{\alpha}{R \sqrt{\rho}} \tag{25}$$

$$R_{xx} = aa^H + I \tag{26}$$

By the matrix inversion lemma

$$R_{xx}^{-1} = I - \frac{aa^H}{1+\rho} \tag{27}$$

where *p* is the optimal output SINR . The updated weight vector $w_{k+1}$is

$$w_{k+1} = R_{xx}^{-1} r_{xd} \tag{28}$$

$$= (I - \frac{aa^H}{1+\rho})(caa^H W_0 + W_0) \tag{29}$$

$$= (\frac{c-1}{1+\rho} aa^H + I)W_0 \tag{30}$$

The output SINR of the updated weight vector is

$$SINR_{k+1} = \frac{|a^H w_1|^2}{w} \tag{31}$$

$$= \frac{\{\rho(\frac{c-1}{1+\rho})+1\}^2 |a^H W_0|^2}{\rho(\frac{c-1}{1+\rho})^2 |a^H W_0|^2 + 2(\frac{c-1}{1+\rho})|a^H W_0|^2 + W_0^H W_0} \tag{32}$$

Since the initial SINR $\rho_0\rho_0$is

$$\rho_0 = \frac{|a^H W_0|^2}{W_0^H W_0} \tag{33}$$

the output SINR of the updated LSCMA weight vector can be written

$$SINR_{k+1} = \frac{\{\rho(\frac{c-1}{1+\rho})+1\}^2 \rho_0}{\rho\rho_0(\frac{c-1}{1+\rho})^2 + 2\rho_0(\frac{c-1}{1+\rho})+1} \tag{34}$$

We argued earlier that the output SINR of the updated LSCMA beamformer is equal to the SINR in the hard limited signal $d_k(n)$ if no background noise is present. It is straightforward to show that

$$\lim_{\rho \to \infty} SINR_{k+1} = c^2 \rho_k = \frac{\alpha^2}{\beta^2} \tag{35}$$

Which supports the argument made earlier. Also note that when c operation provides no gain, and Here the output SINR of the updated weight vector

equals the initial output SINR, as expected.

$$SINR_{k+1}|_{c=1} = \rho_k \quad (36)$$

In order for LSCMA to converge, the hard-limiter must emphasize the desired signal relative to the noise and interference. The effect of hard-limiting and other non-linear operations on communication signals and noise has been a topic of study since the 1950's, e.g., see [17,18] and references therein. A central motivation for this work is to understand the effect of non-linear amplifiers on communication signals, which are commonly used in satellite transponders. Non-linear processing has also been studied as a possible means for reducing the effects of noise and interference, [19,20]. These studies have clearly shown that hard-limiting and filtering a constant envelope signal will increase the SNR, even when the intermodulation components are considered. In fact, for a constant envelope signal, the hard-limiter becomes the optimal nonlinearity as the SNR tends to infinity [21].

A. High SIR

We first examine the situation where the beamformer output SIR is high, as might be the case near LSCMA convergence. We model *y(n)* As

$$y(n) = s(n) + gz(n) = e^{j\varphi(n)} + gm(n)e^{j\psi(n)} \quad (37)$$

where $\varphi(n)$is the phase of the desired signal *s(n),* and *m(n)* and $\psi(n)$ are the magnitude and phase, respectively, of the unit-variance interference term, *z(n).* The scalar *9* controls the SIR, and we assume $g \ll 1$. Note that we have assumed for convenience that the desired signal has unit amplitude in the beamformer output. This has no effect on the behavior of the LSCMA, since any scaling of *y(n)* is removed by hard-limiting The cross-correlation of *s(n)* and *d(n)* is

$$R_{sd} \triangleq \varepsilon\{s(n)\,d^*(n)\} = \varepsilon\{\frac{s(n)\,y^*(n)}{|y(n)|}\} \quad (38)$$

Using the binomial approximation $\frac{1}{|y(n)|} = \frac{1}{\sqrt{y(n)\,y^*(n)}}$,

$$= (1 + g^2m^2(n) + 2gm(n)\cos(\phi(n) - \psi(n)))^{-1/2}$$
$$\cong 1 - gm(n)\cos\Delta(n) \quad (39)$$

where $\Delta(n) = \phi(n) - \psi(n)$ Before proceeding further we consider the PDF of $\Delta(n)$. We are concerned here with the PDF of the phase *difference* of two independent complex baseband signals for the case in which the PDF of the phase of each signal is uniform over *(-π, π].* The desired PDF is obtained by convolving two uniform PDFs, which results in a triangular-shaped PDF over *(-2π, 2π].* Since the phase wraps *($e^{j\Delta} = e^{j2\pi\Delta}$)* the PDF of Δ is uniform over *(-π, π].* This is true even if the received signals have the same modulation format and identical carrier frequencies. The cross-correlation of s(n) and d(n) can now be approximated as

$$R_{sd} \cong \varepsilon\{e^{j\phi(n)}(e^{-j\phi(n)} + gm(n)e^{-j\psi(n)})(1 - gm(n)\cos\Delta(n))\}$$
$$\cong \varepsilon\{(1 + gm(n)e^{j\Delta(n)})(1 - gm(n)\cos\Delta(n))\}$$
$$\cong 1 \quad (40)$$

where the magnitude of the interfering signal m(*n)* and the phase difference ~*(n)* are assumed independent. The result that R_{sd} 1 is intuitively appealing since the SIR is high.

The cross-correlation of *z(n)* and *d(n)* is

$$R_{sd} \cong \varepsilon\{m(n)e^{j\psi(n)}(e^{-j\psi(n)} + gm(n)e^{-j\psi(n)})(1 - gm(n)\cos\Delta(n))\}$$
$$\cong \varepsilon\{(m(n)e^{-j\Delta(n)} + gm^2(n))(1 - gm(n)\cos\Delta(n))\}$$
$$\cong g\varepsilon\{m^2(n)\} - g/2\varepsilon\{m^2(n)\}$$
$$\cong g/2 \quad (41)$$

The output SIR (22) now becomes

$$SIR = \frac{|R_{sd}|^2}{|R_{zd}|^2} = 4g^2 \quad (42)$$

Since the input SIR is 1/ *g2,* the ratio of the output SIR to the input SIR is 4, so that the SIR increases by 6 dB. This result for high SIR holds for any CM signal with uncorrelated cochannel noise and interference and will be observed in the simulation results to follows.

Two Complex Sinusoid Environment

We now examine the behavior of the LSCMA in an environment where the antenna array receives two orthogonal complex sinusoids in the absence of background noise. We show that if the SIR at iteration *k* is known, the LSCMA output SIR can be predicted exactly for all later iterations. We also show that these results are a very good approximation with sinusoids having arbitrary, but well separated, frequencies. The results presented here are deterministic. Other results presented later examine the mean behavior of the LSCMA using a probabilistic framework. The beamformer output signal obtained with the existing LSCMA weight vector is modeled as

$$y(n) = s(n) + gz(n) = e^{jw_1 n} + g\,e^{jw_2 n} \quad (43)$$

where $W_i = 2\pi k_i/N$ for integer k_i. The parameter g determines the relative power of the sinusoids. In Eq.(43),

s(n) and *z(n)* represent the desired signal and the interferer, respectively. The amplitude of the desired signal in *y(n)* is assumed to be unity, which has no effect on the behavior of the LSCMA. Temporal cross-correlation of the desired signal, *s(n),* and the hard-limiter output signal, *d(n)* is

$$\hat{R}_{sd} \triangleq < s(n)d^*(n) >_N = < \frac{1+ge^{j\Delta n}}{|y(n)|} >_N \quad (44)$$

Where $\Delta \triangleq w_1 - w_2$. We note that since *y* is periodic, 1/ |y| is also periodic and may therefore be expressed as a Fourier series. The period of 1/ |y |is 2π/ Δ. The function is real and even, so the Fourier series is given by

$$\frac{1}{|y(n)|} = \frac{a_0}{2} + \sum_{k=1}^{\infty} a_k \cos k\Delta n \quad (45)$$

Where

$$a_k = \frac{2\Delta}{\pi}\int_0^{\pi/\Delta} \frac{cosk\,\Delta n}{\sqrt{1+g^2+2g\,cos\,\Delta n}}\,dn \qquad (46)$$

The Fourier coefficients given by (46) are independent of Δ, which implies that the results to follow hold true for any frequencies W_1 and W_2, if these frequencies lead to orthogonal sinusoids. Substituting (45) into (44) yields

$$\hat{R}_{sd} = < \left(1 + ge^{j\Delta n}\right)\left(\frac{a_0}{2} + \sum_{k=1}^{\infty} a_k\, cosk\,\Delta n\right) >_N \qquad (47)$$

$$= \frac{a_0}{2} + < ge^{j\Delta n} \sum_{k=1}^{\infty} a_k\, cosk\,\Delta n >$$

$$= \frac{a_0}{2} + \frac{ga_1}{2} \qquad (48)$$

The Fourier coefficients a_0 and a_1 may be found using numerical integration. Using a similar approach for $\hat{R}_{ss}$ yields The output SIR of the hard-limiter is

$$SIR_{out} = \frac{|R_{sd}|^2}{|R_{ss}|^2} = \left(\frac{a_0 + ga_1}{ga_0 + a_1}\right)^2 \qquad (49)$$

$$\frac{SIR_{out}}{SIR_{in}} = \left(\frac{a_0 + ga_1}{g\,(ga_0 + a_1)}\right)^2 \qquad (50)$$

and the SIR gain is Figure4 shows the SIR gain (50) as a function of input SIR . Note that the SIR gain tends asymptotically to 6 dB as predicted by the high SIR analysis. The results presented in Figure .4 are now used to predict the output SIR of the LSCMA in an environment containing a sinusoidal desired signal and a sinusoidal interferer. A two element beamformer is simulated with the inter-element spacing equal to one-half the carrier wavelength, A. The desired signal is incident from broadside with an amplitude of one, and the interferer is incident from 30° off broadside with an amplitude of 0.9. The initial LSCMA weight vector is set to $[1\ 0]^T$, so that the initial SIR ≅+0.9 dB. The block size is 1024 samples, with f_1= 5/1024 and f_2 = 31/1024. Table 1 compares the predicted and

measured output SIR at several iterations of the algorithm, which shows excellent agreement with theory. These same results are presented in an alternative manner in Figure5. This figure shows the amplitude of each sinusoid as a function of the number of LSCMA iterations. A similar figure, showing the behavior of the SGD CMA in an environment with two sinusoids, appears in [10].

We now briefly consider the case in which the two complex sinusoids are not orthogonal. The cross-correlation between the two sinusoids will be small if the two sinusoids are well separated in frequency. For this case we would expect the preceding analysis to be a good approximation to the observed behavior. This is supported by the results shown in Table 2. The simulation parameters are the same as in Table 1, except that f_1= 0.5/1024 and f_2 = 3/1024. The agreement with theory is still very good even though the sinusoids are not orthogonal.

C. CM Signal with CM Interference

We now consider an environment where the antenna array receives a CM desired signal and a CM interferer in the absence of background noise.

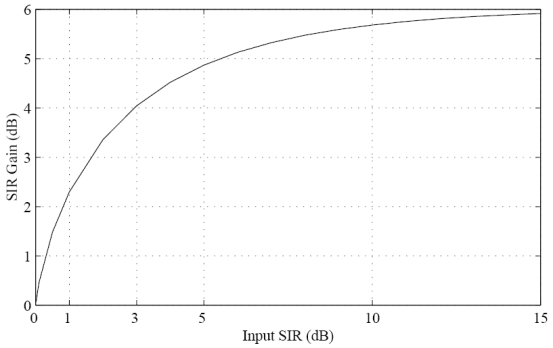

Figure 4: Improvement in SIR achieved by one iteration of LSCMA with sinusoidal desired signal and sinusoidal interferer.

Unlike the deterministic framework employed in the sinusoidal environment, we now rely on a probabilistic framework. These results therefore describe the mean behavior of the LSCMA. The initial beamformer output signal *y(n)* is modeled as

$$y(n) = e^{j\phi(n)} + ge^{j\psi(n)} \qquad (51)$$

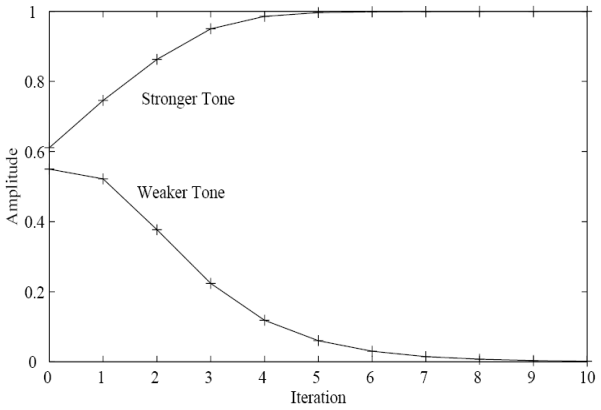

Figure5: Amplitude of both complex sinusoids in the beamformer output as a function of the number of LSCMA iterations. Solid line indicates predicted amplitude, '+' indicates amplitude measured in simulation.

Table 1: Comparison of predicted and measured LSCMA output SIR in an environment containing two complex sinusoids.

Iteration	Output SIR (dB)		SIR Gain
	Measured	Theory	
0	0.915	0.915	-
1	3.097	3.095	2.181
2	7.195	7.193	4.099
3	12.554	12.552	5.358
4	18.390	18.388	5.837
5	24.363	24.361	5.973
6	30.372	30.370	6.009
7	36.389	36.387	6.018
8	42.409	42.407	6.020

where $\varphi(n)$ and $\psi(n)$ denote the phase of the desired signal and interfering signal, respectively, and g determines the relative power.

We assume that $\varphi(n)$ and $\psi(n)$ are independent random variables uniformly distributed over $[-\pi, \pi]$. The cross-correlation of the desired signal $s(n)$ and the hard-limiter output signal $d(n)$ is,

$$R_{sd} = \int_{-\pi}^{\pi} \frac{1+ge^{j\Delta}}{\sqrt{1+g^2+2g\cos\Delta}} p(\Delta)\, d\Delta \qquad (52)$$

where $\Delta \triangleq \varphi\Delta \triangleq \varphi(n) - \psi\psi(n)$ $p(\Delta) = 1/2\pi p(\Delta) = 1/2\pi$ $-\pi < \Delta \leq \pi - \pi < \Delta \leq \pi$. We simplify the expression for $R_{sd}R_{sd}$ by noting that $e^{j\Delta}e^{j\Delta} = \cos\Delta\Delta + j\sin\Delta\Delta$, and odd functions when integrated over $-\pi\pi$ to $\pi\,\pi$ yield zero. We thus obtain

$$R_{sd} = \frac{1}{2\pi}\int_{-\pi}^{\pi} \frac{1+g\cos\Delta}{1+g^2+2g\cos\Delta}\, d\Delta$$
$$R_{sd} = \frac{1}{2\pi}\int_{-\pi}^{\pi} \frac{}{\sqrt{1+g^2+2g\cos\Delta}}\, d\Delta \qquad (53)$$

Similarly, the cross-correlation of the interferer $z(n)$ and the hard-limiter output signal can be expressed as

$$R_{zd} = \frac{1}{2\pi}\int_{-\pi}^{\pi} \frac{g+\cos\Delta}{g^2+2g\cos\Delta}\, d\Delta$$
$$R_{zd} = \frac{1}{2\pi}\int_{-\pi}^{\pi} \frac{}{\sqrt{1+g^2+2g\cos\Delta}}\, d\Delta \qquad (54)$$

Table 2: Comparison of predicted and measured LSCMA output SIR in an environment containing two complex sinusoids when the sinusoids are not orthogonal.

Iteration	Output SIR (dB)		SIR Gain
	Measured	Theory	
0	0.915	0.915	-
1	3.084	3.095	2.17
2	7.119	7.193	4.035
3	12.358	12.552	5.239
4	18.054	18.388	5.697
5	23.885	24.361	5.831
6	29.752	30.370	5.867
7	35.627	36.387	5.876
8	41.505	42.407	5.878

The SIR Eq.(22) is calculated by evaluating both Eq.(53) and Eq.(54) by numerical integration. The resulting SIR gain is shown in Figure 6. The expected gain of hard-limiting in this environment is identical to the deterministic gain achieved in the sinusoidal signal environment. The mean SIR gain measured from simulation when the LSCMA is applied to an environment containing two FM signals with low-pass Gaussian messages is also shown in the Figure 6. The array configuration and AOA of the signal and interference are the same as those used previously in the sinusoidal environment. The signals are generated by low-pass filtering Gaussian noise to a normalized bandwidth of 0.125, and then frequency modulating using a frequency deviation of 0.1. The baseband FM signals have no carrier frequency offset. The mean SIR gain is measured from 1000 Monte Carlo trials using $N = 256$ samples. Figure.6 shows excellent agreement between the theoretical and measured SIR gain. As further evidence of the applicability of the above derivation to other CM modulation formats, we apply LSCMA to an environment with two QPSK signals. In order for the QPSK signals to be CM, we assume that they have the same symbol timing, and that they have been appropriately match-filtered and sampled baud-synchronously.

We also assume that the QPSK signals have no carrier frequency offset. Thus each QPSK signal takes on one of four values which are drawn randomly from the set $\{\pm 1/\sqrt{2}, \pm i/\sqrt{2}\}$. The carrier phase of each QPSK signal is randomly drawn from a uniform distribution for each trial. Simulation results are shown in Figure 7. All simulation parameters are the same as those used in the FM signal environment. Once again, there is excellent agreement between the predicted and observed behavior of LSCMA.

In most practical applications, PSK signals with non-rectangular pulse shape are used in order to reduce the signal bandwidth. Unless the PSK signal is appropriately match-filtered and sampled baud synchronously it will not be CM. Accurate estimation of symbol timing is difficult in the presence of strong co-channel interference. However, this is precisely the sort of environment where adaptive beam forming would be applied. Thus the preceding assumption that the desired QPSK signal is sampled baud synchronously will not be valid in general. One solution to this problem is to apply the LSCMA to oversampled data, i.e., sample the digital signal at a rate higher than the symbol rate, since the CMA can be applied to non-constant modulus signals [4]. The symbol timing can be re-estimated as the

Multipliers	Present study	[3]	[6]
Technology (nm)	70	70	70
Transistor counts	24213	26135	28531
Multiplication time (ns)	3.4	4.4	4.2
Chip Area (mm^2)	0.55	0.67	0.72
Power Diss. (mW)	0.54	0.63	0.67

Figure 6. Improvement in output SIR achieved with one iteration of LSCMA with an FM desired signal and an FM interferer. Solid line indicates theoretical gain, '+' indicates mean gain measured in simulations.

LSCMA converges. Ultimately the LSCMA can be adapted using only the baudsynchronous (constant modulus) samples instead of the oversampled (non-constant modulus) data. The analysis framework described here can be used to determine the performance of the LSCMA with pulse-shaped PSK signals. However, such an analysis is beyond our scope, and we instead rely on simulation to gain some insight into this issue. We would expect

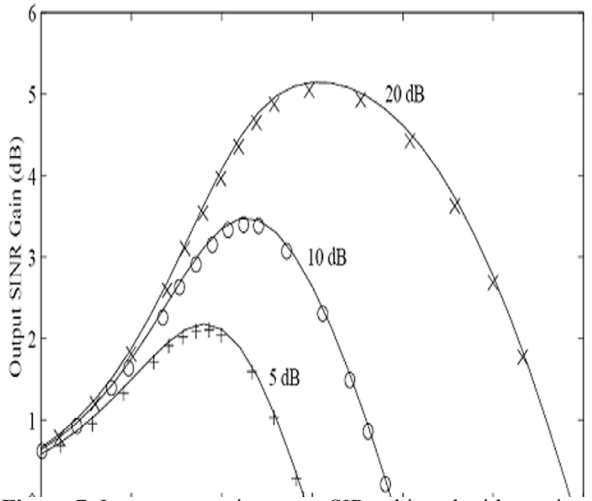

Figure 7. Improvement in output SIR achieved with one iteration of LSCMA with a QPSK desired signal and a QPSK interferer. Solid line indicates theoretical gain, '+' indicates mean gain measured in simulations.

that the LSCMA will still converge with a pulse-shaped QPSK signal, but that the convergence will be slower. We examine the behavior of LSCMA with two pulse-shaped 1f /4 QPSK signals. This modulation is commonly used in cellular and PCS applications. The signals are sampled at 8 times It is well known that signals having lower excess bandwidth have higher modulus variation. Thus we would expect LSCMA to converge more quickly with higher excess bandwidth signals. This is verified by Figure 8, which shows the SIR gain for both 20% and 100% excess bandwidth. The simulation parameters used to generate these results are the same as those used previously. The SIR gain for the 100% excess bandwidth signal appears to asymptotically approach ≈ 4.7 dB as the initial SIR becomes high. The SIR gain for the 20% excess bandwidth signal appears to approach ≈3.9 dB as the initial SIR becomes high. These results indicate that the LSCMA will converge more slowly with a non-constant modulus signal than with a CM signal

D. CM Signal with Gaussian Interference

We now examine the behavior of the LSCMA with a CM signal and Gaussian interference. These results are of interest since the distribution of a large number of co-channel interferers, as might be encountered in CDMA applications, will tend toward Gaussian by the central limit theorem. The input to the hard-limiter is expressed as :

$$y(n) = s(n) + gz(n) = e^{j\phi(n)} + gm(n)e^{j\psi(n)} \quad (55)$$

where *s(n)* is an angle-modulated signal and *z(n)* is unit-variance complex Gaussian interference. Note that $\psi(n)$is uniformly distributed over *(-π, π]*while *m(n)* is Rayleigh distributed with PDF:

$$r(m) = \begin{cases} 2me^{-m^2} & m > 0 \\ 0 & m < 0 \end{cases} \quad (56)$$

The cross-correlation of *s(n)* and *d(n)* is

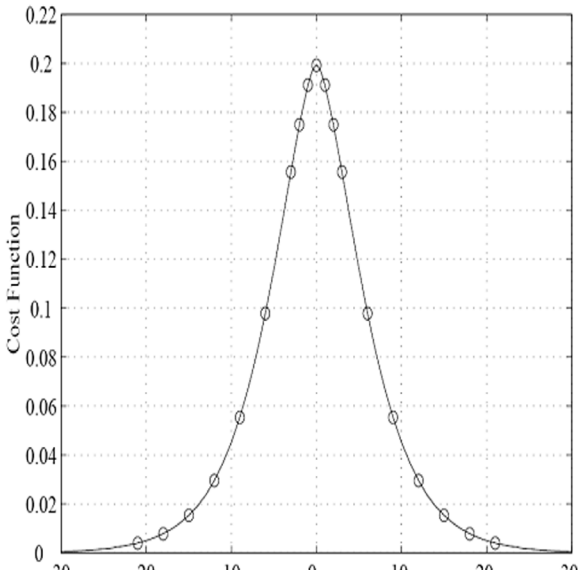

Figure 8. SIR gain of LSCMA with non-constant modulus pulse-shaped 1f /4 QPSK signals. The results are parametric in the percent of excess bandwidth for each signal. The dotted curves are based on Monte Carlo simulation, the solid curve is the theoretical result for a CM desired signal with CM interference. the symbol rate, and Nyquist-type pulse shaping is used.

$$R_{sd} = \frac{1}{\pi}\int_0^{\infty} Q(m)\ me^{-m^2} dm \quad (57)$$

Where

$$Q(m) = \frac{1}{2\pi}\int_{-\pi}^{\pi} \frac{1+gmcos\Delta}{\sqrt{1+g^2m^2+2gmcos\Delta}} d\Delta \quad (58)$$

In a similar fashion it can be shown that

$$R_{zd} = \frac{1}{\pi}\int_0^{\infty} P(m)\ me^{-m^2} dm \quad (59)$$

Where $P(m) = \frac{1}{2\pi}\int_{-\pi}^{\pi} \frac{mcos\Delta+gm^2}{\sqrt{1+g^2m^2+2gmcos\Delta}} d\Delta$ (60)

Both Eq.(57) and Eq.(59) are evaluated by numerical integration and used to obtain the SIR gain shown in Figure 9. The SIR gain as measured from simulations is also shown in Figure 9 and verifies the theoretical analysis. The simulation parameters are the same as those used previously. As before the SIR gain tends to 6 dB as the input SIR becomes high. Note that the SIR gain is greater than 0 dB even for an input SIR of -10 dB. This would seem to indicate that

LSCMA can be expected to converge even at low initial input SIR. However, it is important to bear in mind that these results are based on probabilistic notions. The SIR gain will be a random variable for finite block size and Figure 9 shows only the expected value of this random variable.We have now calculated α and β for several important signal and interference distributions. At this point we have sufficient information to study the (1,2)-CMA cost function using these expressions for α and β.

Cost Function Analysis

In order to perform a thorough analysis of any blind algorithm, it is necessary to find the stationary points of the cost function. A stationary point occurs when the gradient with respect to the weight vector is equal to zero. These stationary points are important because they correspond to local minima, local maxima, or saddlepoints of the cost function.

The gradient of a blind cost function with respect to the weight vector cannot, in general, be solved for directly. If this could be accomplished, the weight vector that minimizes the cost function could be solved for directly without the need for iterative algorithms. However, it is sometimes possible to express the cost function in terms of the output SINR and other parameters as opposed to the weight vector. This can simplify the analysis. for the (1,2) CMA cost function

$$F(\rho) = 2 - \frac{2}{\sqrt{1+\rho}}(\alpha^* \sqrt{\rho} + \beta^*) \quad (61)$$

where α and β are as defined earlier, and p is the beamformer output SINR. Note that a and jJ are dependent on the SINR ρ. Figure 10 shows the (1,2) CMA cost function as calculated from Eq.(61) for the case of a CM signal and CM interference. Simulation results are included to support the analytic results. These simulation results are based on a CM signal and a CM interferer. The signal and interference are white, and the phase in each case is random and uniformly distributed. The (1,2) CMA cost function was measured with a data length of 1024 samples, and averaged over 1000 independent Monte Carlo trials.

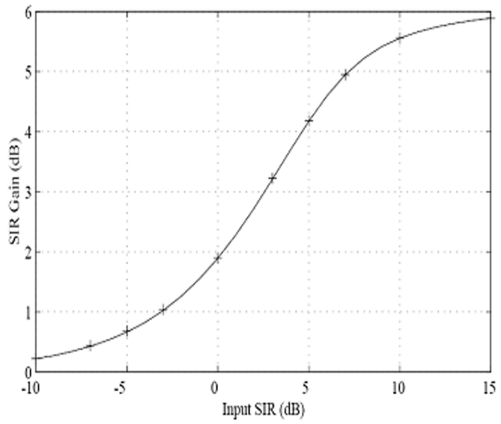

Figure 9. Improvement in output SIR achieved with one iteration of LSCMA for a CM signal plus Gaussian interference. Solid line indicates theoretical gain, '+' indicates mean gain measured in simulations with an FM signal and a Gaussian interferer.

Note that the cost function in Figure 10 is symmetric about a dB SIR. This is to be expected, since the CMA cost function cannot distinguish between a CM signal and a CM interferer. Also note that the cost function has a global maximum at a dB SIR. Since the gradient is small in the neighborhood of a dB SIR, a gradient search algorithm, such as steepest descent, will converge slowly in this environment if the initial SIR is low. Figure 11 shows the (1,2) CMA cost function as calculated from Eq.(61) for the case of a CM signal and Gaussian noise and interference. Simulation results are again included to support the analytic expression Eq.(61). The simulation parameters are identical to those used previously, except that the noise is complex Gaussian as opposed to CM. As expected, the cost function grows small as the SIR grows large. However, the

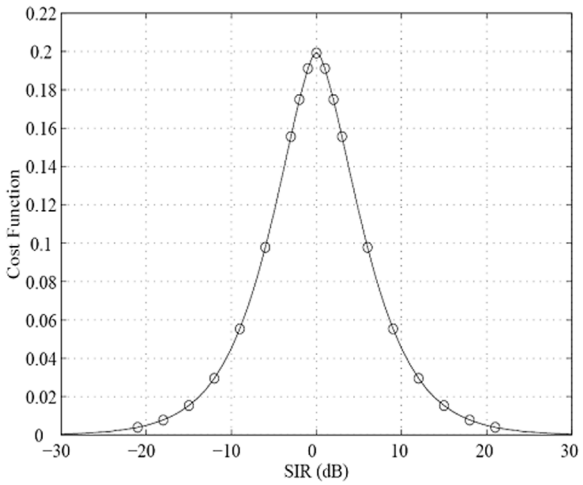

Figure 10. (1,2) CMA cost function versus SIR with a CM signal and CM interference. The solid line shows the analytic expression, the '0' show simulation results.

behavior for low SIR is very different for Gaussian noise than for CM noise. In Gaussian noise, the cost function remains large, but the gradient approaches zero as the SIR grows small. Since a gradientbased algorithm seeks to find a point in the cost function where the gradient is zero, a gradient-based CMA may become trapped in a low output SIR state. This is known as *noise capture* .In noise capture, the output of a CMA-adapted array consists of Gaussian background noise; any CM signals received by the array are nulled.

Inclusion of Background noise

In this section we examine the effect of background noise on the behavior of the LSCMA. We assume that the noise has a complex circularly symmetric Gaussian distribution and is uncorrelated from sensor to sensor. We consider one environment where the interference is Gaussian, and another where the

interference is CM. In both cases the desired signal is QPSK and is assumed to have been match filtered and sampled so that it is CM. All simulation results are based on 1000 trials with the LSCMA block size equal to 256 symbols. The array is linear with eight

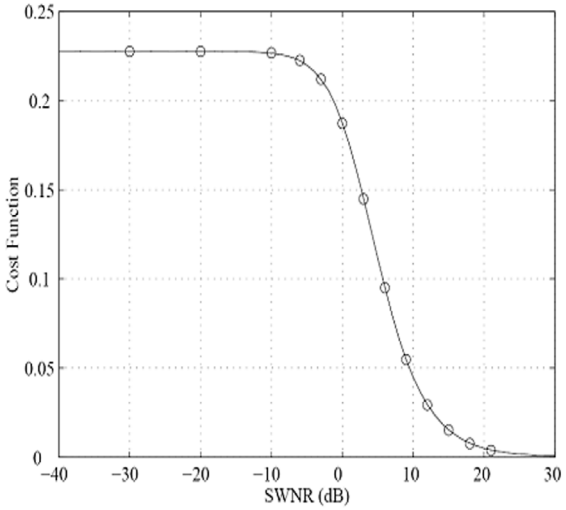

Figure 11. (1,2) CMA cost function versus SIR with a CM signal and Gaussian interference. The solid line shows the analytic expression, the '0' show simulation results

elements and uniform interelement spacing equal to $\lambda/2$. The signal power is measured relative to the unit variance background noise, and is termed the Signal to White Noise Ratio (SWNR).

First consider the case where the desired signal is incident from 0° and a single Gaussian interferer is incident from 5°. Since the noise and interference is Gaussian, the SINR gain from hard-limiting is given by Eq.(57) and Eq.(59). The LSCMA output SINR is related to the SINR gain from hard-limiting by Eq.(34). The mean LSCMA SINR gain is presented

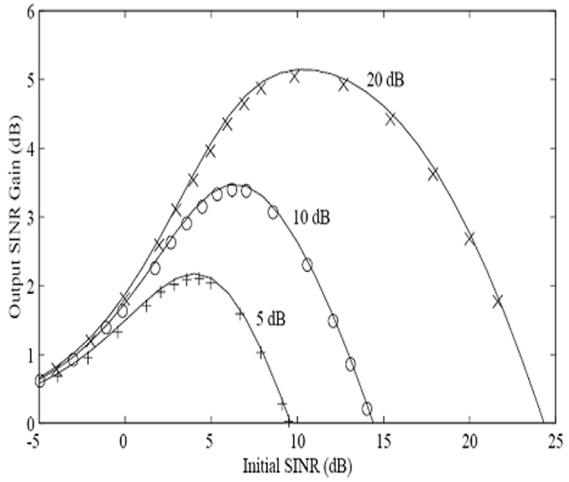

Figure 12. Improvement in output SIR achieved with one iteration of LSCMA with a QPSK desired signal received with a Gaussian interferer and Gaussian background noise. Solid lines indicate theoretical result, '+','0', and 'x' denote mean gain from simulation.

in Figure 12 for SWNR equal to 5, 10, and 20 dB. The power of the interferer is kept equal to the power of the desired signal. The figure shows excellent agreement between the measured and predicted SINR gain. As the SWNR increases, the optimal output SINR increases, and the SINR gain approaches the gain obtained when no background noise is present. Now consider the case where the interference is CM. Since the interference is not Gaussian, calculation of the SINR gain is tedious and it is appropriate to make some approximations. When the beamformer output SINR is low, the dominant source of distortion is the CM interferer, and the SIR gain from hard-limiting can be accurately predicted by the results for CM interference, given by Eq.(53) and Eq.(54). As the output SINR becomes higher, the interferer is nulled, and the background noise becomes the dominant source of distortion. However, we have shown that in all cases the SINR gain from hard-limiting approaches 6 dB as the SINR becomes high. Therefore the behavior of LSCMA in this case can be predicted by using the results for CM interference Eq.(53) and Eq.(54) together with Eq.(34). Simulation results for an environment similar to that described above, except that the Gaussian interferer is replaced with a CM QPSK interferer, are presented in Figure.13.This figure shows very good agreement between the approximate theoretical result and the simulation results.

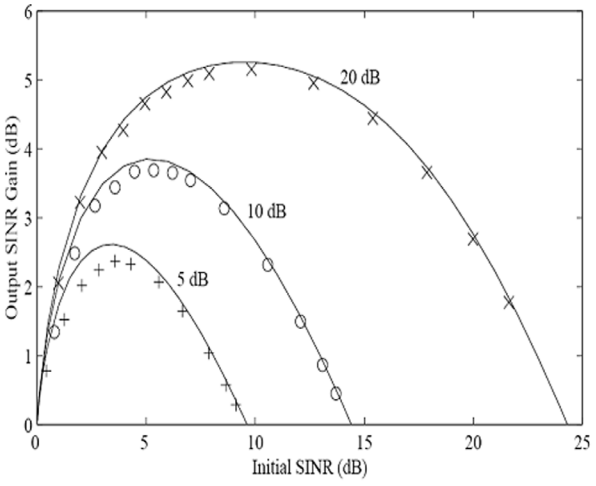

Figure 13. Improvement in output SIR achieved with one iteration of LSCMA with a QPSK desired signal received with a QPSK interferer and Gaussian background noise. Solid lines indicate theoretical result, '+','0', and 'x' denote mean gain from simulation.

Finite Block Size

The effect of finite block size on classical least squares beam forming (with a known training signal) has been considered previously [22]. While it should be possible to apply some of these same techniques to the analysis of the LSCMA, we instead rely on simulation to obtain some intuition regarding the

effect of finite block size. The mean behavior of the LSCMA should be very close to that predicted by the analysis, even for small block size. Furthermore the variance of the SIR gain should decrease with increasing block size. This is verified by Figure 14, which shows the distribution of SIR gain versus the LSCMA block size with an FM desired signal and an equal power Gaussian interferer. The results are based on 1000 trials. Note that a significant number of trials had SIR gain of less than 0 dB, i.e., the Gaussian interferer was emphasized. The LSCMA will not converge to the desired solution in these cases, but will instead capture the Gaussian interferer. However, for block sizes of 64 samples and higher, no trials were observed to have negative SIR gain. Thus the algorithm tends to behave in the

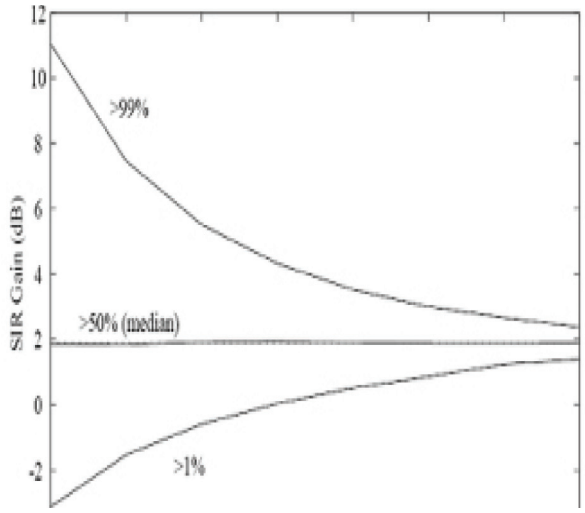

Figure 14. SIR gain of LSCMA versus block size with an FM desired signal and a dB Gaussian interferer. Dotted line indicates theoretical gain. Upper and lower traces define region where 98% of trials fell.

desired manner as the block size increases. Proper selection of the initial weight vector can also help ensure LSCMA convergence to the desired solution.

CONCLUSION

We have examined the convergence behavior of the LSCMA in some simple environments. The results are derived by calculating the improvement in SIR caused by hard-limiting a CM signal plus additive noise and interference. These results help to explain why LSCMA converges, and are helpful in explaining the general behavior of LSCMA. However, we have made several simplifying assumptions which must be addressed in order to extend the analysis to more realistic situations. We have assumed that the desired signal and the interfering signals are not correlated. This does not in general allow the direct analysis of correlated multipath environments. However, the analysis presented here is valid for the case where the multi path delay spread is very small. In this case, the delayed paths are highly correlated with the desired path, and the overall effect is simply to change the spatial signature. Many applications require the extraction of multiple signals. Algorithms such as Multi Target CMA, Multistage CMA, and Iterative Least Squares with Projection can be used for this purpose. The results presented here can form a basis for analysis of these multi-signal extraction techniques. Clearly the variance and distribution of output SINR obtained with the LSCMA is also an important area for investigation. We finally comment on the hard-limit non-linearity. For high SIR, the hard-limiter is the optimal non-linearity when the desired signal has a constant envelope. However, at low SIR other non-linearities can yield greater SIR gain. Thus it is possible that non-linear functions other than the hard-limit can be used to develop blind adaptive algorithms which converge faster for low initial SINR.

Acknowledgements

This work was supported by Islamic azad university of Urmia the Department of Young Researchers Club Urmia branch(YRC) and university of urmia. Authors would like to thank YRC and university of Urmia for their financial support.

REFERENCE

[1] D.C. Youla and H. Webb, "Image restoration by the method of convex projections:Part I, theory", *IEEE Trans. Medical Imaging,* vol. MI-1, pp. 81-94, Oct. 1982.

[2] R. Gooch and J. Lundell, "The CM array: An adaptive beamformer for constant modulus signals", *Proc. of Inter. Conf. on Acous., Speech, and Signal Process.,* pp. 2523-2526, April 1986.

[3] J. R. Treichler and B. G. Agee, "A new approach to multipath correction of constant modulus signals", *IEEE Trans. on Acous., Speech, and Signal Process.,* vol. ASSP-31, no. 2, pp. 459-471, April 1983.

[4] J. Lundell and B. Widrow, "Application of the constant modulus adaptive beamformer to constant and nonconstant modulus signals", *Proc. of the Asilomar Conf. on Signals, Systems, and Computers,* pp. 432-436, Nov. 1987.

[5] Y Wang, YC. Pati, YM. Cho, A. Paulraj, and T. Kailath, "A matrix factorization approach to signal copy of constant modulus signals arriving at an antenna array" , *Proc. of the 28th Conf. on Information Science and Systems (Princeton, NJ),* pp. 178-183, Mar. 1994.

[6] H.J. Trussell and M.R. Civanlar, "The feasible solution in signal restoration", *IEEE Trans. on Acous., Speech, and Signal Process.,* vol. ASSP-32, no. 2, pp. 201-212, April 1984.

[7] Henry Stark, Ed., *Image Recovery - Theory and Application,* Academic Press, 1987. [71] D.C. Youla, "Generalized image restoration by the method of alternating projections", *IEEE Trans. on Circuits Syst.,* vol. CAS-25, pp. 694-702, Sept. 1978.

[8] A.L. Swindlehurst, S. Daas, and J. Yang, "Analysis of a decision directed beamformer", *IEEE Trans. on Signal Processing.,* vol. 43, no. 12, pp. 2920-2927, December 1995.

[9] Z. Kostic, M.L Sezan, and E.L. Titlebaum, "Estimation of parameters of a multipath channel using set-theoretic deconvolution", *IEEE Trans. on Commun.,* vol. 40, no. 6, pp. 1006-1011, June 1992.

[10] J. R Treichler and M. G. Larimore, "The tone capture properties of CMA-based interference suppressors", *IEEE Trans. on Acous., Speech, and Signal Process.,* vol. ASSP-33, no. 4, pp. 946-958, August 1985.

[11] T. E. Biedka, "A comparison of initialization schemes for blind adaptive beam forming", *Proc. of Inter. Conf. on Acous., Speech, and Signal Process.,* pp. 1665-1668, May 1998.

[12] RW. Gerchberg and W.O. Saxton, "A practical algorithm for the determination of phase from image and diffraction plane pictures", *Optik,* vol. 35, no. 2, pp. 237-246, 1972.

[13] B. G. Agee, "The least-squares CMA: A new technique for rapid correction of constant modulus signals", *Proc. of Inter. Conf. on Acous., Speech, and Signal Process.,* pp. 953-956, April 1986.

[14] Alle-Jan van der Veen and A. Paulraj, "An analytical constant modulus algorithm", *IEEE Trans. Signal Processing,* vol. 44, no. 5, pp. 1136-1155, May 1996.

[15] Z. Ding, RA. Kennedy, B.D.O. Anderson, and C.R Johnson, Jr., "Ill-convergence of Godard blind equalizers in data communication systems", *IEEE Trans. on Commun.,* vol. 39, no. 9, pp. 1313-1327, Sept. 1991.

[16] Y Li and Z. Ding, "Convergence analysis of finite length blind adaptive equalizers", *IEEE Trans. Signal Processing,* vol. 43, no. 9, pp. 2120-2129, Sept. 1995.

[17] N.M. Blachman, "Detectors, bandpass nonlinearities, and their optimization: Inversion of the Chebyshev transform", *IEEE Trans. on Information Theory,* vol. IT-17, no. 4, pp. 398-404, July 1971.

[18] N.M. Blachman, "The output signal-to-noise ratio of a bandpass limiter", *IEEE Trans. on Aerosp. and Electronic Systems,* p. 635, July 1968.

[19] K.J. Friederichs, "A novel canceller for strong CW and angle modulated interferers in spread spectrum receivers", *Proc. of IEEE Military Commun. Conf.,* pp. 32.4/1-4, Oct 1984.

[20] YC. Pati, G.G. Raleigh, and A. Paulraj, "Estimation of co-channel FM signals with multitarget adaptive phase-locked loops and antenna arrays", *Proc. of Inter. Conf. on Acous., Speech, and Signal Process.,* pp. 1741-1744, May 1995.

[21] N.M. Blachman, "Optimum nonlinearities and pessimum interference", *Proc. of the Second Workshop on Cyclostationary Signals,* pp. 5.1-9, Aug. 1994.

[22] 1. S. Reed, J. D. Mallett, and L. E. Brennan, "Rapid convergence rate in adaptive arrays", *IEEE Trans. Aerospace Electron. Syst.,* vol. AES-10, pp. 853-863, Nov. 1974.